



Seasonal Variability and Cloud-Type Effects on Secondary Organic Aerosol Formation During Cloud Events at a Mountainous Site in Southeastern China

Yi Zhang^{1,2}, Weiqi Xu^{1,2}, Yan Li^{1,2}, Guohua Zhang³, Dantong Liu⁴, Ye Kuang⁵, Yu Zhang^{1,2}, Wei Zhou^{1,2},
Xiaocong Peng³, Bojiang Su³, Weihong Huang⁵, Zijun Zhang^{1,2}, Liu Yang^{1,2}, Yangzhou Wu^{4,6}, Siyuan
Li⁴, Shitong Zhao⁴, Lanzhong Liu⁷, Xiaole Pan^{1,2}, Zifa Wang^{1,2}, Xinhui Bi³, Mikael Ehn⁸, Douglas R.
Worsnop^{8,9}, Yele Sun^{1,2}

¹State Key Laboratory of Atmospheric Environment and Extreme Meteorology, Institute of Atmospheric Physics, Chinese Academy of Sciences, Beijing 100029, China

²College of Earth and Planetary Sciences, University of Chinese Academy of Sciences, Beijing 100049, China

³State Key Laboratory of Advanced Environmental Technology, Guangzhou Institute of Geochemistry, Guangzhou Institute of Geochemistry, Chinese Academy of Sciences, Guangzhou 510640, China

⁴Department of Atmospheric Sciences, School of Earth Sciences, Zhejiang University, Hangzhou 310058, China

⁵Institute for Environmental and Climate Research, Jinan University, Guangzhou 511143, China

⁶College of Environmental Science and Engineering, Guilin University of Technology, Guilin 541006, China

⁷Shanghuang Atmospheric Boundary Layer and Eco-Environment Observatory, Institute of Atmospheric Physics, Chinese Academy of Sciences, Jinhua 321203, China

⁸Institute for Atmospheric and Earth System Research/Physics, Faculty of Science, University of Helsinki, Helsinki 00140, Finland

⁹Aerodyne Research Inc., Billerica, MA 01821, USA

Correspondence to: Weiqi Xu (xuweiqi@mail.iap.ac.cn) and Yele Sun (sunyele@mail.iap.ac.cn)

Abstract. Aerosol-cloud interactions exert substantial influences on atmospheric chemistry and regional climate, yet real-time characterization of chemical and microphysical evolution within cloud droplets remain limited. Here, two intensive campaigns were conducted at the high-altitude Shanghuang station in southeastern China during autumn 2023 and spring 2024, capturing distinct nocturnal orographic and long-persistence stratiform cloud events. Using a ground-based counterflow virtual impactor and an aerosol-cloud sampling inlet system along with integrated aerosol chemical speciation and cloud microphysical measurements, we resolved the composition of interstitial (INT), and residual (RES) particles during cloud events and ambient particles (AMB) under cloud-free conditions. Organic aerosols (OA) dominated particle mass across both seasons, while inorganic species (nitrate, sulfate, ammonium) exhibited high scavenging efficiencies ($\geq 65\text{--}70\%$) and strong enrichment in RES particles. Organic components showed seasonally contrasting partitioning patterns. Organics in INT particles exhibited a lower degree of oxidation during orographic clouds in 2023, whereas those in RES particles were more oxidized. In contrast, persistent clouds in 2024 displayed the opposite behaviour, reflecting shifts in aqueous-phase oxidation. Air-mass analysis further revealed pronounced source-dependent variability, with polluted westerly inflow leading to the highest particle loadings and most aged organic signatures. By linking chemistry with microphysics, we found that secondary organic aerosol formation preferentially occurs in smaller droplets, while OA from primary emissions is more efficiently incorporated into larger droplets



through collision-coalescence. These results provide a quantitative, process-level understanding of seasonal and cloud-type controls on in-cloud chemical evolution, offering new constraints for representing aqueous-phase processing in atmospheric models.

1 Introduction

40 Clouds play a pivotal role in regulating the Earth's radiative balance and exert a profound influence on global climate through both the back-scattering of solar radiation and the modulation of terrestrial infrared emission (Twomey, 1974; Haywood and Boucher, 2000). Nevertheless, despite notable advances in understanding cloud–climate interactions, recent Intergovernmental Panel on Climate Change (IPCC) assessments underscore that clouds remain the dominant source of uncertainty in overall climate feedback (Forster et al., 2021). This persistent uncertainty is largely attributable to the intrinsic complexity of cloud
45 processes, which arise from the intricate coupling between microphysical evolution and multiphase chemical transformations. The microphysical and chemical properties of cloud droplets vary substantially with cloud altitude, cloud type, lifecycle stage, and even seasonal conditions, and are further modulated by the influence of anthropogenic emissions. (Pan et al., 2023; Zhao et al., 2022; Yeom et al., 2025; McCoy et al., 2020; Li et al., 2020a). Consequently, online in-situ measurements of both cloud microphysical parameters and the chemical composition of cloud droplets are indispensable. Such observations provide a more
50 holistic characterization of the dynamic evolution of cloud droplet chemistry and offer critical insights into its coupling with cloud microphysical processes.

The chemical composition of atmospheric particles during cloud events is shaped by a complex interplay of factors, including gaseous precursors, air mass origins, cloud classifications, cloud altitudes, cloud life-cycle stages, and seasonal meteorological regimes (Bi et al., 2016; Adachi et al., 2022; Zipori et al., 2015; Graham et al., 2020; Sun et al., 2025). Current understanding
55 highlights several dominant mechanisms underlying aerosol-cloud interactions, such as the scavenging of aerosol particles by nucleation and impaction processes, the collision–coalescence and aqueous-phase processing occurring within clouds, and the activation of hygroscopic particles to form cloud droplets (Seinfeld et al., 1998). Together, these mechanisms modulate aerosol size distributions, chemical partitioning, and oxidative evolution throughout the cloud cycle (Hoppel et al., 1986; Elperin et al., 2008; Pierce et al., 2015). Nevertheless, despite extensive conceptual frameworks, a quantitative characterization of how
60 distinct stages of cloud evolution, particularly cloud formation, mature cloud development, and cloud dissipation, differentially influence individual aerosol components remains insufficiently constrained. Moreover, the response of organic aerosol species to cloud processing, especially under varying cloud types and seasonal conditions, is still poorly understood. These knowledge gaps hinder a mechanistic interpretation of cloud-mediated chemical aging and limit our ability to accurately represent cloud–aerosol interactions in atmospheric models.

65 High-altitude stations, due to their unique geographical characteristics, serve as ideal sites for studying regional and orographic clouds. As shown in Fig. S1, extensive cloud-related field observations have been conducted at mountain stations worldwide



over the past few decades (Lawrence et al., 2023; Hutchings et al., 2009; Hill et al., 2007; Graham et al., 2020; Li et al., 2020b; Liu et al., 2025). Among previous observations, the dominant method for investigating the chemical composition of cloud droplets has been offline sampling (Demoz et al., 1996) combined with laboratory analysis (Igawa and Wang, 2022; Sun et al., 2023; Hutchings et al., 2009). For example, Li et al. (2017) utilized the Caltech Active Strand Cloud Water Collector (CASCC) to collect cloud droplet samples at Mount Tai in eastern China to examine inorganic ions, organic carbon, and organic acids in cloud water. Similarly, Sun et al. (2024) employed the CASCC to collect cloud droplets at Mt. Tianjing in southern China and applied the Positive Matrix Factorization (PMF) method to apportion the sources of cloud-water chemical species. In addition to offline approaches, several techniques have been developed to enable real-time characterization of cloud droplets (Lawrence et al., 2023; Gao et al., 2023). Among them, the GCVI has emerged as a key instrument capable of automatically identifying cloud events and actively separating cloud droplets from INT aerosols. By coupling the GCVI with a high-resolution aerosol mass spectrometer and other online instruments at Mt. Daming, Shen et al. (2025) demonstrated that RES particles exhibit enhanced hygroscopicity due to their higher nitrate content, and observed a representative cloud episode in which hygroscopic INT particles efficiently absorbed ambient water vapor, thereby limiting further droplet growth. Despite these advances, real-time, in-situ measurements of the chemical composition of both cloud droplets and INT aerosols remain exceedingly limited. This poses a significant challenge to fully resolving the dynamic chemical–microphysical interactions within cloud systems and underscores the need for more comprehensive observational datasets from high-altitude platforms.

To address these gaps, we conducted two intensive field campaigns at a high-altitude station, capturing multiple orographic cloud and long-persistence cloud events across contrasting seasons. By employing two complementary cloud-droplet sampling systems, i.e., GCVI and custom-designed aerosol-cloud sampling inlet system (ACSIS), integrated with an aerosol chemical speciation monitor and concurrent cloud microphysical measurements, this study provides the real-time characterization of organic and inorganic aerosol evolution throughout cloud formation and dissipation in this region. Specifically, we examine the influence of air-mass origins on aerosol chemical composition during cloud events, the wet scavenging and in-cloud processing of particle chemical components, and the dependence of organic aerosol partitioning and oxidation on cloud microphysical parameters such as Liquid water content (LWC), D_e , and N_c . The resulting insights contribute to a more detailed, process-level understanding of aerosol–cloud interactions in orographic cloud and long-persistence cloud environments and help constrain their representation in chemistry–climate models.

2 Materials and Methods

2.1 Sampling site

Two field campaigns were conducted from 16 September to 21 October 2023 and from 17 April to 1 June 2024 at the summit of Mt. Damaojian (119.51°E, 28.58°N; 1128 m above sea level), at the Shanghuang Eco-Environmental Observatory of the Chinese Academy of Sciences (hereafter, SH). This site is a forested location in southeastern China, where the ambient atmosphere is predominantly influenced by local biogenic emissions, with a comparatively minor contribution from anthropogenic sources (Zhang et al., 2024a; Wang et al., 2025). The region is characterized by a subtropical monsoon climate,



100 and our sampling period coincided with the transition between the wet and dry season. Consequently, cloud events occurred frequently during the observation period (Fig. S2), providing favourable conditions for investigating the characteristics and evolution of aerosol components and organic components during cloud processing.

2.1.1 Cloud droplet and aerosol sampling systems

In the two field campaigns, two different sampling approaches were employed for particle selection and sampling. In the autumn of 2023, cloud events were identified using the GCVI installed on the roof of the observation station under the following conditions: ambient visibility below 3 km, relative humidity (RH) exceeding 95%, and absence of precipitation. When a cloud event occurs, the GCVI would automatically identify meteorological conditions and separate cloud droplets with diameter larger than 8.7 μm (lower cut size). These droplets are subsequently introduced into the evaporation chamber, where they are dried by an air flow maintained at 40 $^{\circ}\text{C}$ (Bi et al., 2016; Shingler et al., 2012). The resulting dried particles, referred to as RES particles, are then directed toward further analysis. An enrichment factor of 6.68, determined by the tunnel airflow, sample flow, and inlet geometry, was applied to correct for the particle concentration enhancement inherent to the CVI inlet, which causes particles in cloud droplets in the sampled air to be enriched relative to that in ambient air (Guo et al., 2025; Shingler et al., 2012). Simultaneously, INT particles were alternately sampled using a $\text{PM}_{2.5}$ cyclone throughout the duration of several cloud events, following a 30-minute alternating sampling cycle. Under cloud-free conditions, only particles with aerodynamic diameters smaller than 2.5 μm were collected, denoted as AMB particle.

In 2024, the ACSIS sequentially switched between the PM_1 impactor, $\text{PM}_{2.5}$ impactor, and total suspended particles (TSP) every 15 minutes (Kuang et al., 2024). To maintain sample inlet RH below 20% throughout the field campaigns, AMB particles and droplets were dried using a Nafion dryer. RES particles were defined as those not captured by the $\text{PM}_{2.5}$ impactor but detected in the TSP passage during cloud events, while INT were defined as those through by the $\text{PM}_{2.5}$ impactor.

2.1.2 Measurements of particle chemical composition and microphysical properties

A Time-of-Flight Aerosol Chemical Speciation Monitor (ToF-ACSM; Aerodyne Research Inc., USA) equipped with a capture vaporizer and $\text{PM}_{2.5}$ aerodynamic lens and a seven-wavelength Aethalometer (AE33; Magee Scientific Corp., USA) were connected with the end of GCVI or ACSIS to measure non-refractory particles species including organics (Org), sulfate (SO_4), nitrate (NO_3), ammonium (NH_4), chloride (Chl), and equivalent black carbon (BC). The time resolution of the measurements is 2 and 1 min, respectively. For microphysical parameters of cloud droplets, a fog monitor (FM-100; Droplet Measurement Technologies, USA) was used to optically measure diameter size and number concentration of cloud droplets with size ranging from 2 to 50 μm . The instrument resolves particles into 30 size bins, and the size ranges of every bin vary for different sizes, with 1 μm -resolution for droplets smaller than 14 μm and 2 μm -resolution for droplets bigger ones. The time resolution of FM-100 is 1 sec. LWC, the total number concentration (N_t), effective diameter (D_e) and volume-mean diameter (D_v) of cloud droplets were determined as previous studies (Ding et al., 2025).



2.1.3 Meteorological measurements

Meteorological parameters including temperature (T) and RH were measured by a T /RH probe (HC2S3; Campbell Scientific Inc., USA). The hourly wind speed (WS) and wind direction (WD) in 2023 were obtained from European Reanalysis 5 reanalysis dataset, and they were measured by MetOne 034B in 2024. The ambient concentration of $PM_{2.5}$ and CO were measured using a continuous ambient particulate monitor (Model 5014i; Thermo Scientific., USA) and Picarro green-house gas analyzer (G2401; Picarro Inc., USA), respectively.

2.2 Data Analysis

2.2.1 ACSM calibration and source apportionment

The mass concentrations of non-refractory particles species were analyzed using ACSM standard data analysis software (Tofware_v2.5.13_ACSM). The default relative ionization efficiencies (RIEs) of 1.1, 1.4 and 1.3 were applied for nitrate, organics and chloride, and the RIEs values of ammonium and sulfate were 3.5 and 1.2 according to the ionization efficiency calibration using pure NH_4NO_3 (NH_4) $_2$ SO_4 particles. To determine the sources and atmospheric oxidation processes of OA, the multilinear engine algorithm (ME-2) was used for source apportionment of OA for ACSM datasets in 2023 and 2024 (Paatero, 1999). The mass spectral profiles of isoprene-epoxydiol-derived secondary OA (IEPOX-SOA) measured at the same forested site in July 2024, characterized by relatively high contributions of marker ions f_{82} (1.24%) and f_{81} (1.05%) (commonly used as tracers for IEPOX-SOA), were constrained by varying the a -value from 0 to 1 (Hu et al., 2018; Hu et al., 2015). This approach accounts for the inherent production of IEPOX-SOA at forested sites, which is typically associated with elevated biogenic emissions. Four OA factors, including primary OA (POA), IEPOX-SOA, less oxidized oxygenated OA (LO-OOA), and more oxidized oxygenated OA (MO-OOA) with an a -value of 0.2 were identified in 2023 and 2024. IEPOX-SOA contributed 7.2%-9.3% of OA on average, consistent with the previous results in forest sites (Hu et al., 2015). The POA mass spectrum is dominated by prominent hydrocarbon ions (for example, m/z 41, m/z 43, m/z 55, and m/z 57), and the ratio of m/z 55 and 57 (2.95 in 2023 and 1.82 in 2024) are similar to those determined from ToF-ACSM with capture vaporizer (Zheng et al., 2020; Xu et al., 2020). Additionally, both LO-OOA and MO-OOA exhibit distinct m/z 44, consistent with observations across multiple sites in previous studies (Lei et al., 2021; Joo et al., 2021; Sun et al., 2022). Compared with OA factors in winter (Zhang et al., 2024b), MO-OOA is more correlated with sulfate in autumn ($R^2=0.91$, Fig. S3) and spring ($R^2=0.77$, Fig. S4) due to stronger aqueous-phase oxidation processing and regional transport. Moreover, the moderate correlation between LO-OOA and nitrate ($R^2=0.85$) in 2024 suggested their possibly similar formation pathways. The three-factor ME-2 solution produced a mixed SOA factor, while the five-factor solution further decomposed the two SOA factors into three distinct components. However, these additional components remain uninterpretable due to insufficient external tracers.

2.2.2 Feasibility of GCVI and ACSIS measurements

Considering that two distinct cloud-droplet sampling systems were employed across the two field campaigns, we conducted a preliminary assessment of the droplet size distribution associated with each system (Fig. S5). During the orographic cloud events in autumn 2023, cloud droplets exhibited relatively large D_v , with maxima reaching $\sim 27 \mu m$. Under such conditions,



the GCVI, whose lower cut size is approximately 8.7 μm , successfully captured about 80 % of the cloud droplet population. In contrast, during the persistent cloud episodes in 2024, droplet sizes predominantly ranged from 3 to 9 μm , a regime that can be effectively sampled by the ACSIS. This indicates that, despite the use of different cloud droplet sampling systems in the two campaigns, both approaches successfully captured the vast majority of cloud droplets present in the ambient atmosphere. These complementary size-capture efficiencies indicate that the measurements obtained in the two years are highly comparable.

2.2.3 Scavenging efficiency

To quantify the wet scavenging process of different chemical components in the cloud process at the SH site, scavenging efficiency of major chemical components (η_i) was calculated based on mass concentration change of $\text{PM}_{2.5}$ during cloud formation stage (Noone et al., 1992; Gilardoni et al., 2014). Cloud formation stage is defined as the first few hours when visibility had stabilized below 100 meters. The calculation formula is as follows:

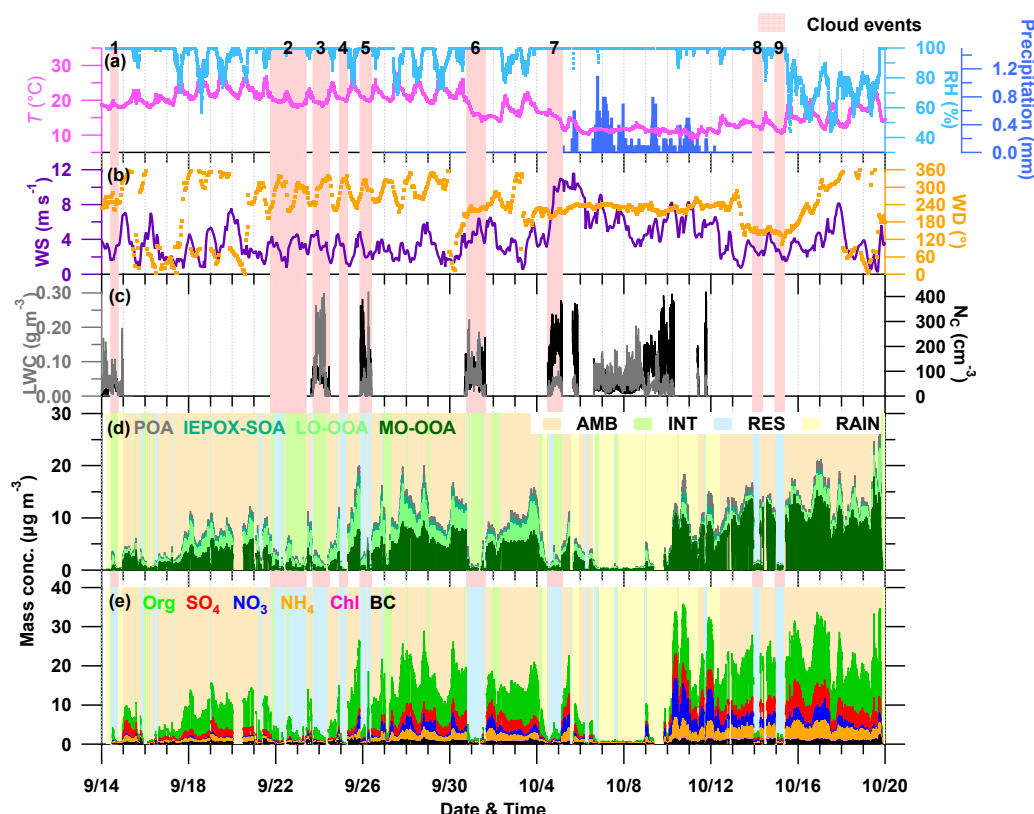
$$\eta_i = 1 - \frac{c_{INT}^i}{c_{AMB}^i}, \quad (4)$$

where c_{INT}^i and c_{AMB}^i represent the mass concentrations of i species in INT particles and pre-cloud AMB particles, respectively. The i species include Org, SO_4 , NO_3 , NH_4 , Chl, BC, POA, IEPOX-SOA, LO-OOA, and MO-OOA.

3 Results and Discussion

3.1 Overview of field campaigns in 2023 and 2024

Figure 1 presents the time series of meteorological variables, cloud microphysical parameters, and the organic and inorganic chemical components of aerosol particles observed during the autumn of 2023. Throughout this observational period, nine distinct cloud events were identified, among which five enabled successful concurrent sampling of RES and INT particles (Table S1). The unique geographical and topographical characteristics of the mountainous site resulted in pronounced diurnal variability in meteorological conditions. As solar radiation declined after sunset, air temperature progressively decreased, leading to a reduction in the saturation vapor pressure and elevated RH levels during nighttime (Fig. S6). The sustained low temperatures and high RH (reaching 100%) at night facilitated the formation and persistence of cloud processes. As a result, cloud events at this site typically occurred between 20:00 and 08:00 throughout the observation period. The clouds formed under such conditions at the mountain site are classified as orographic clouds. Furthermore, the mass concentrations of both INT and RES particles exhibited a marked decrease relative to those of AMB particles prior to the onset of cloud events.



190 **Figure 1: Overview of the measurements during the field campaign in 2023. (a, b) Meteorological parameters, (c) LWC and N_c , (d) OA factors, (e) particles compositions. The red-shaded area represents the cloud events, while the background shading in panels (d) and (e) corresponds to ambient (AMB), interstitial (INT), residual (RES), and rain (RAIN) periods, shown in orange, green, blue, and yellow, respectively.**

Compared with the observations in autumn 2023, the cloud processes that occurred in spring 2024 exhibited distinct meteorological and microphysical characteristics. During the spring of 2024, seven cloud events were observed. Aerosol particles were successfully collected throughout each cloud events, enabling the quantification of the mass concentrations of chemical components within cloud droplets (RES) by calculating the differences between TSP and PM_{2.5} measurements. In contrast to the cloud processes observed in autumn 2023, those in spring 2024 were predominantly characterized by remarkable persistence, often lasting for several tens of hours and frequently accompanied by rainfall, therefore classified as long-persistence cloud events (Table S2). As a consequence, the diurnal variation in cloud occurrence probability displayed a relatively smooth and continuous pattern (Fig. S6). Moreover, the diurnal cycles of T and RH during the spring 2024 observation period were more pronounced than those in autumn 2023, with lower nighttime temperatures and noticeably drier daytime conditions. Due to the influence of wet scavenging, the PM_{2.5} mass concentration decreased substantially throughout the cloud events.

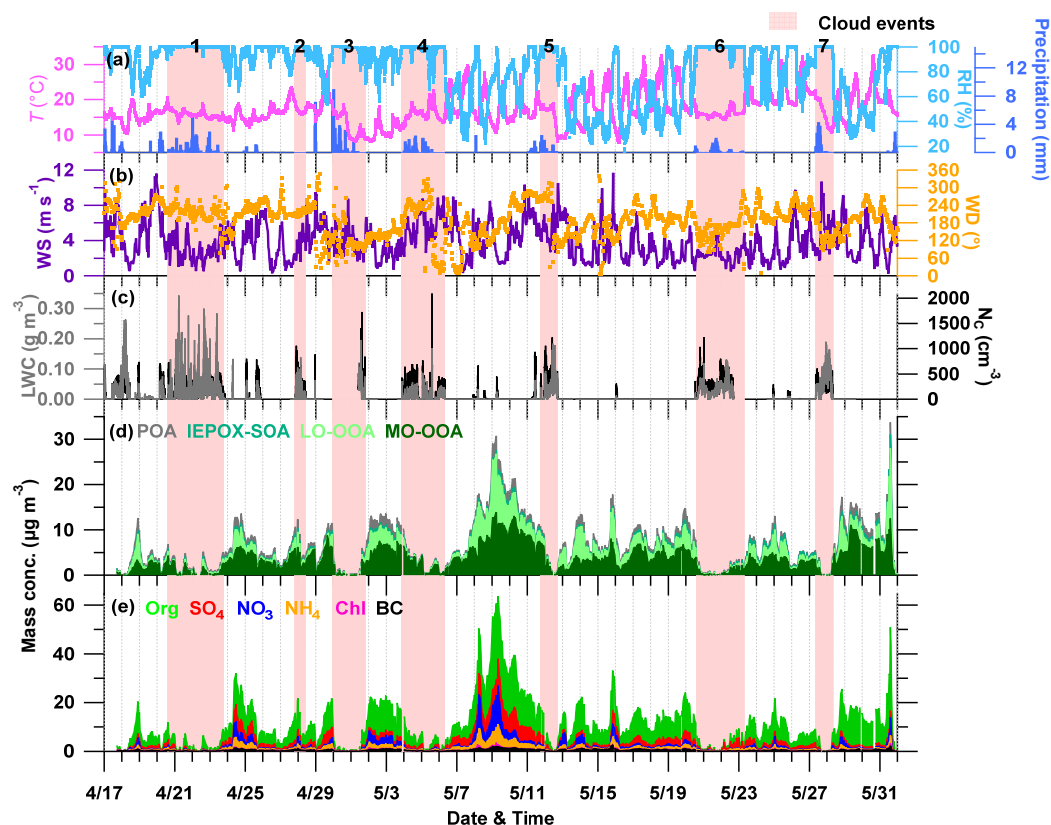


Figure 2: Overview of the measurements during the field campaign in 2024. (a, b) Meteorological parameters, (c) LWC and N_c , (d) OA factors, (e) chemical compositions of $PM_{2.5}$ particles during the entire campaign. The red-shaded area represents the cloud events.

Figure 3 presents the average mass concentrations and relative contributions of chemical components in different types of particles during the cloud processes observed in both campaigns. The chemical composition of RES, INT, and pre-cloud AMB particles was dominated by organics, which accounted for more than 55% of the total mass. Compared with the observations conducted at the Daming Mountain site in spring 2023 (Shen et al., 2025), the organic fraction at SH was slightly higher, likely due to the differences in regional emission sources. The organic mass fraction in ambient particles decreased by approximately 4.4-17% after the cloud processes, consistent with the results obtained during the previous campaign at the same site (Zhang et al., 2024b). Relative to the pre-cloud AMB particles, the mass fractions of nitrate and ammonium increased substantially in RES particles during both observation periods, whereas the less hygroscopic BC exhibited a noticeable enrichment in INT particles. A key difference between the two campaigns was observed in the behaviour of sulfate. During the orographic cloud events in autumn 2023, the sulfate contribution decreased in both INT and RES particles, while during the long-persistence cloud events in spring 2024, its fraction showed a slight increase in both types of particles. This suggests that prolonged cloud processing can enhance the secondary formation of sulfate (Guo et al., 2025).

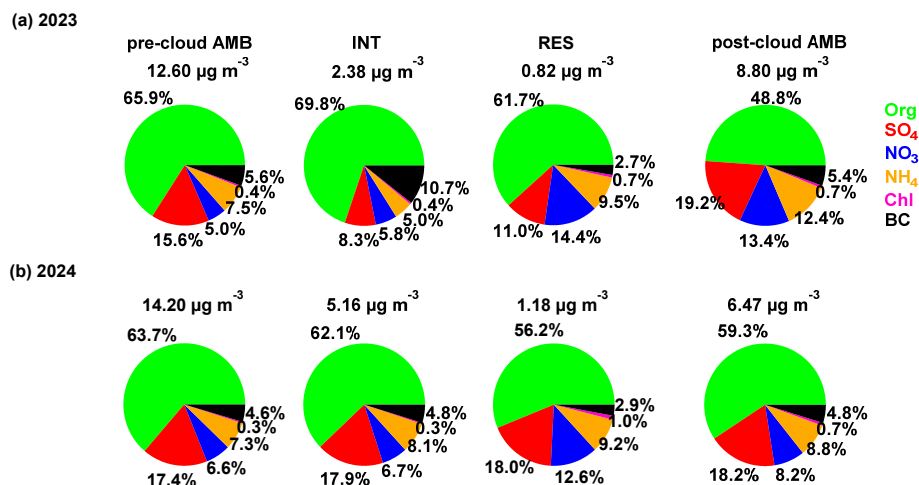
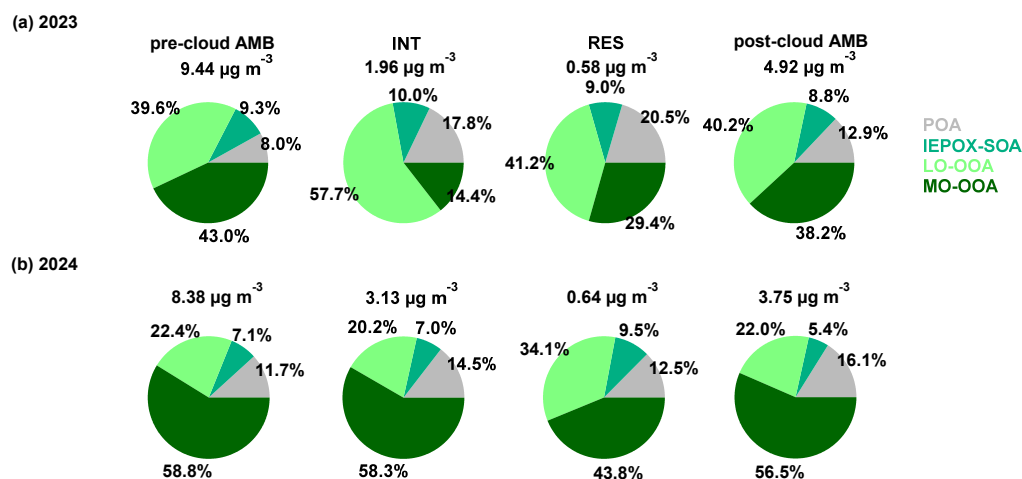


Figure 3: Average chemical composition of different types of particles (pre-cloud AMB, INT, RES and post-cloud AMB) in (a) 2023 and (b) 2024.

The organic components of different particle types exhibited pronounced variability (Fig. 4). As shown by the spectral comparison of LO-OOA and MO-OOA (Fig. S7), the ME-2 resolved OA factors exhibit strong interannual consistency, with F44 values remaining closely aligned for both LO-OOA (0.34 vs. 0.27) and MO-OOA (0.34 vs. 0.36). Across all four particle types observed during the two campaigns, SOA predominated, accounting for more than 79.5% of the total organic mass.

Compared with the particles sampled in 2023, those collected in 2024 were generally more aged, characterized by a higher proportion of MO-OOA (44 – 59%). For the two particle types associated with cloud processes, INT and RES particles, the relative contributions of LO-OOA and MO-OOA exhibited distinct differences between the two observation periods. During the typical nocturnal orographic cloud events in autumn 2023, the fraction of LO-OOA in INT particles was higher than that in RES particles, whereas the opposite pattern was observed for MO-OOA. In contrast, during the long-persistence cloud processes in spring 2024, INT particles contained a higher fraction of MO-OOA, consistent with the results obtained at the same site in 2022, while RES particles exhibited a relatively larger contribution from LO-OOA. These results indicate that the oxidation pathways of organics within particles differ markedly between nocturnal orographic clouds and continuous long-lasting cloud events. Short-lived orographic clouds tend to facilitate moderate oxidation of organics in INT particles and deeper liquid oxidation in RES particles, whereas prolonged cloud processing appears to reverse this pattern. Detailed comparisons between the two observation periods are provided in Table S3.



240 **Figure 4: Average organic aerosol composition of different types of particles (pre-cloud AMB, INT, RES and post-cloud AMB) in (a) 2023 and (b) 2024.**

3.2 Impact of different air mass sources on particle composition

To investigate the influence of air mass origins on the chemical composition of particles at the SH site, backward trajectories of air masses during the cloud events were calculated for both observation periods (Fig. S8). Taking the results from autumn
 245 2023 as an example, the nine cloud events observed during the campaign can be broadly classified into three categories based on their air mass origins: cases 1- 5 originated from the east and mainly passed over the ocean; cases 6 and 7 were affected by a typhoon system, with air masses arriving predominantly from the north; and cases 8 and 9 were transported from the west, primarily passing over the continental regions of China.

Figure 5 shows the variations in the chemical composition of different particle types under the influence of air masses from
 250 these different source regions in autumn of 2023. Air masses from the east, which were relatively less influenced by anthropogenic emissions, were associated with the lowest total mass concentrations of pre-cloud AMB, post-AMB and RES particles, as well as the lowest organic mass concentrations. These air masses also exhibited the highest organic mass fractions (71.6%) with the organics characterized by the lowest degree of oxidation, as indicated by a smaller proportion of MO-OOA. In contrast, air masses transported from the west were strongly influenced by intensive anthropogenic emissions, resulting in
 255 the highest total mass concentrations of AMB particles among the three air mass categories. Specifically, the mass concentration of pre-cloud AMB particles associated with western air masses was approximately 2.6 times higher than that observed in eastern air masses and 1.3 times higher than that in northern air masses. These western air masses also contributed to the highest total mass concentrations of chemical components in RES particles with a marked increase in the fraction of aged organics, where MO-OOA exceeded 65% in both RES and INT particles. The results in 2024 also reached a similar
 260 conclusion (Fig. 6).

The variations in chemical composition associated with different air mass origins can be largely attributed to the combined effects of emission characteristics and atmospheric processing during transport. For air masses originating from the east, long-range transport over the marine boundary layer likely resulted in efficient wet scavenging and dilution, leading to lower overall particle mass and a dominance of less oxidized organic matter (Gantt and Meskhidze, 2013; O'dowd et al., 2004). The relatively low oxidation state of organics in these air masses suggests limited photochemical aging during transport, consistent with the shorter transport pathways and cleaner upwind environments. In contrast, air masses arriving from the west were subject to substantial influences from continental pollution sources, particularly from industrial and urban regions in eastern China. During their long-range transport, these air masses underwent extensive multiphase and photochemical processing, promoting the secondary formation and aging of organic aerosols. As a result, the fraction of MO-OOA increased markedly in RES particles. The enhanced sulfate contribution observed in these cases further indicates that aqueous-phase oxidation processes in RES particles may have been more active under the higher pollution loadings associated with continental air masses. Overall, these findings highlight that regional air mass sources play a crucial role in determining the abundance and chemical evolution of cloud-related particles at the SH site.

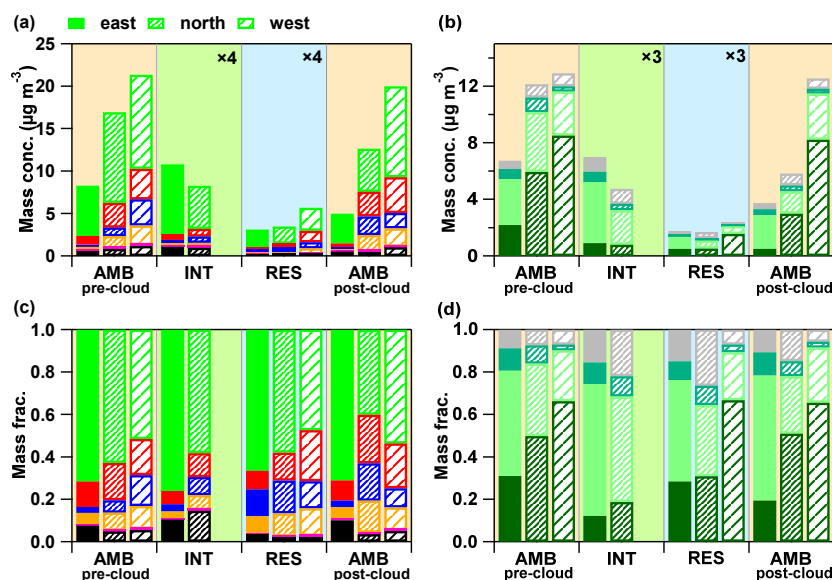


Figure 5. (a, b) Mass concentrations and (c, d) mass fractions of four types of particles (pre-cloud AMB, INT, RES and post-cloud AMB) influenced by air masses from different sources (east, north, west) during the 2023 observation period.

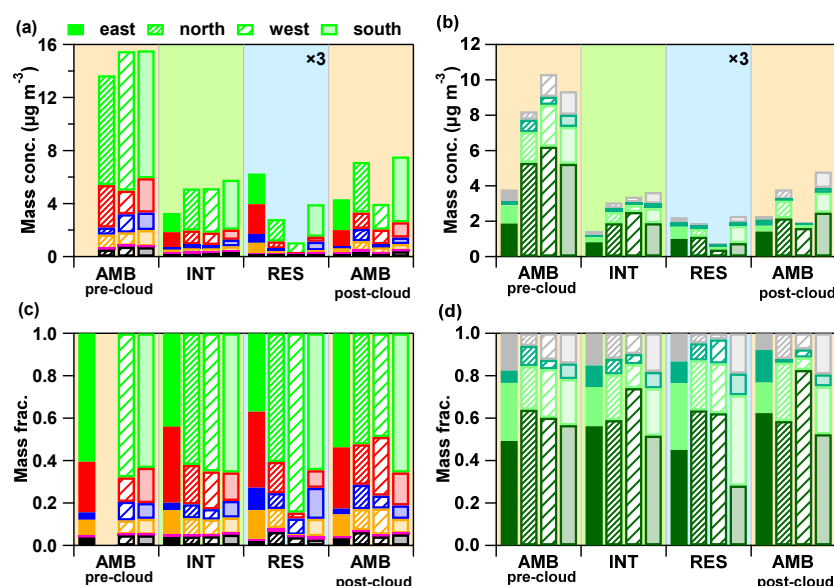


Figure 6. (a, b) Mass concentrations and (c, d) mass fractions of four types of particles (pre-cloud AMB, INT, RES and post-cloud AMB) influenced by air masses from different sources (east, north, west) during the 2024 observation period.

3.3 The variability of chemical components during cloud processes

3.3.1 Wet scavenging and contributions of chemical components in RES particles

Wet scavenging plays a crucial role in influencing AMB particles, during cloud events, acting as the primary mechanism for aerosol removal from the atmosphere. The scavenging efficiency varies depending on chemical compositions of the aerosols. Figure 7a illustrates the scavenging efficiencies of various chemical species during cloud formation in the two field campaigns. Cloud formation is defined as the initial hours when visibility dropped below 100 meters, with specific event details summarized in Table S1. In both campaigns, inorganic components exhibited consistently high scavenging efficiencies, with average values exceeding 65% in autumn 2023 and 70% in spring 2024. These results are comparable to those reported by Gilardoni et al. (2014) in the Po Valley, yet higher than those observed by Zhang et al. (2020) during fog events in a U.S. forested park. The scavenging efficiency of organics was generally similar to that of nitrate. Among organic components, SOA were more efficiently scavenged than POA during both observation periods, likely due to the lower hygroscopicity of POA. This behaviour was also observed for BC, which showed limited removal efficiency. Among the four organic components identified, MO-OOA showed the highest wet scavenging efficiency, followed by IEPOX-SOA, consistent with their respective hygroscopic properties. The average values of scavenging efficiencies for different chemical components in the two campaigns are summarized in Table S4.

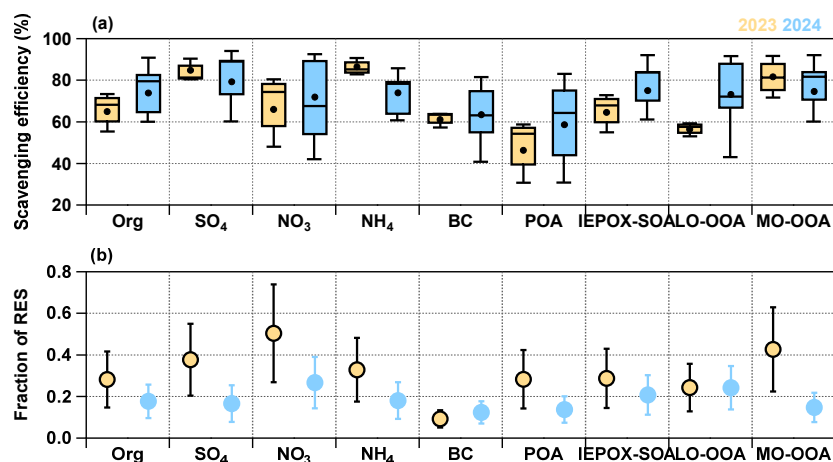


Figure 7: (a) Scavenging efficiency of chemical components in 2023 and 2024. (b) Average fraction of chemical components in RES particles (RES / (RES+INT)) during cloud events in 2023 and 2024.

Figure 7b presents the fractional distribution of different chemical species within RES particles during cloud events. Overall, nitrate, sulfate, and ammonium accounted for a larger proportion in RES particles, suggesting that these three inorganic species were more actively produced within clouds than other components (Guo et al., 2025). This phenomenon can also be attributed to their high hygroscopicity, which facilitates their activation and incorporation into cloud droplets. Regarding the organic components, MO-OOA exhibited a higher fraction in RES particles during the topographic cloud processes in autumn 2023 than other organic species, implying that the vigorous liquid-phase oxidation occurring within RES particles enhanced the aging of organic matter. This elevated fraction can also be explained by its high hygroscopicity, which facilitates its activation into cloud droplets and thus promotes its preferential incorporation into RES particles (Chen et al., 2017; Deng et al., 2018). These two processes, strong in-cloud oxidative processing and enhanced activation due to high hygroscopicity, jointly contributed to the elevated proportion of MO-OOA observed in RES particles during the 2023 topographic cloud events.

However, during the more persistent cloud events in spring 2024, LO-OOA exhibited the highest fractional contribution in RES particles compared with the other three factors. The observed seasonal differences in the fractional composition of organics within RES particles were closely related to the microphysical properties of clouds (Fig. 8). In contrast, during the spring 2024 cloud events, the average LWC of cloud droplets was 49.2% lower and the D_e was 38.4% smaller than those observed in autumn 2023. Such microphysical conditions suggest that smaller cloud droplets may favor the formation of moderately oxidized organic species, while simultaneously suppressing the progression toward more highly oxidized organics due to the limited extent of liquid-phase oxidation within smaller droplets. This interpretation is further discussed in Sect. 3.4. A similar pattern can be seen when comparing different cloud events. For instance, between cases 4 and 7 in 2024, case 4 exhibited both lower fractional contributions of chemical species within the RES particles and reduced LWC and D_e during the cloud period (Figs. S10 and S11).

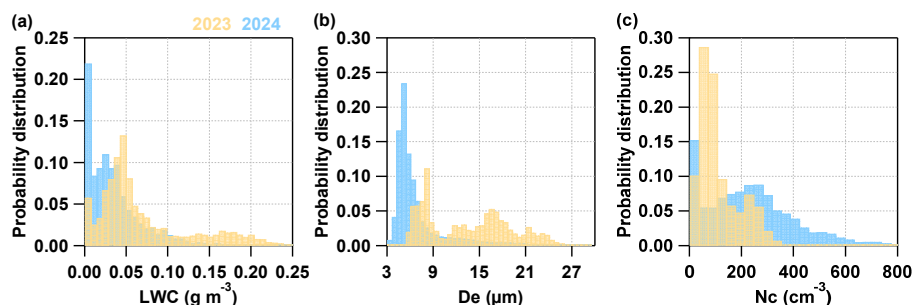


Figure 8: Average probability distribution of (a) LWC, (b) D_e and (c) N_c during the cloud periods in 2023 and 2024.

3.3.2 Chemical composition changes during cloud formation and dissipation

To further investigate the compositional changes of different chemical species in particles during cloud formation and dissipation, we compared the variations in the fractional contributions of chemical components between INT and AMB particles, as well as between RES and AMB particles for both observation campaigns (Fig. 8). During the cloud formation stage, we compared in-cloud INT / RES particles with the pre-cloud AMB aerosols, while during the cloud dissipation stage, we compared the post-cloud AMB particles with the in-cloud INT / RES particles. Cloud formation is defined as in Sect. 3.3.1, and the cloud dissipation stage is considered as the final hours of the cloud event when visibility remained consistently below 100 m. As shown in the Fig. 9, the variation patterns of particle chemical composition during the cloud formation stage were generally consistent between autumn 2023 and spring 2024. Organics, particularly POA, together with the less hygroscopic BC, exhibited higher fractions in INT particles, whereas nitrate and ammonium were enriched in RES particles. Such compositional shifts associated with cloud formation have also been reported by Mattsson et al. (2025) and Zhang et al. (2022). However, the evolution of organic components differed between the two observation periods. During the autumn 2023 campaign, LO-OOA was preferentially enriched in INT particles during the cloud formation stage, while MO-OOA accumulated in RES particles. These changes reversed during the cloud dissipation stage, leading to only minor differences in the fractional contributions of secondary organics in the post-cloud AMB particles (Figs. 8a and b). In contrast, during the spring 2024 campaign, the fraction of LO-OOA in RES particles increased by 20.1% relative to that in pre-cloud AMB particles during the cloud formation stage, and the LO-OOA fraction in ambient particles further increased by 5.22% during cloud dissipation (Figs. 8c and d). This indicates that during long-lasting cloud events, LO-OOA formed within cloud droplets can be released back into the atmosphere upon cloud evaporation (Zhang et al., 2024b), thereby altering the organic composition of ambient aerosols. These findings highlight the critical role of cloud microphysical processes in regulating the redistribution and transformation of SOA within and after cloud events.

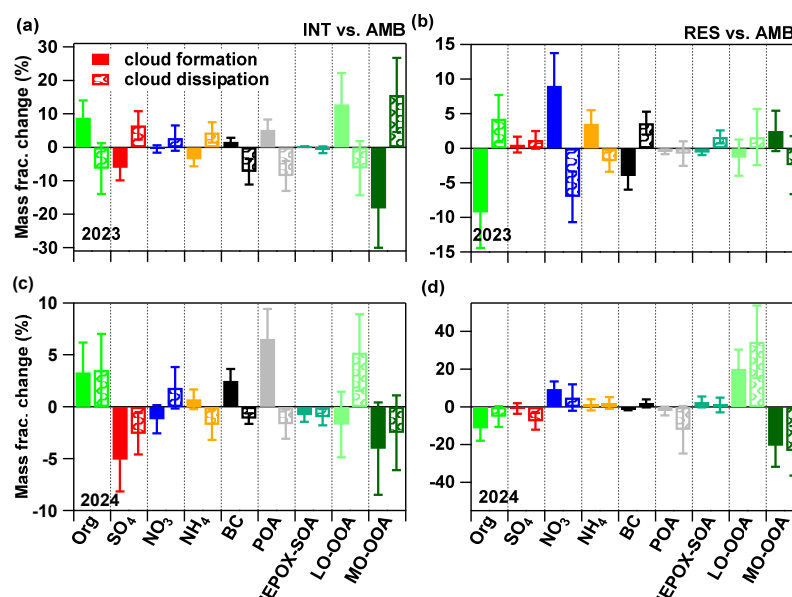


Figure 9: Mass fraction changes of chemical species between INT and AMB particles during cloud formation and dissipation in (a) 2023 and (c) 2024, and changes between RES and AMB particles in (b) 2023 and (d) 2024.

3.4 Evolution of in-cloud organic components under different cloud microphysical properties

To further investigate the variation characteristics of organics within cloud droplets, two representative cloud events in 2023 and one in 2024 was selected. The variations in the fractional contributions of organic components and the total mass concentration of organics with respect to cloud microphysical parameters were analyzed (Fig. 10). During the selected events in 2023, the mass fraction of LO-OOA in RES particles increased as the LWC and D_e decreased, whereas the fraction of POA showed an opposite trend, increasing with higher LWC and D_e . In contrast, IEPOX-SOA exhibited little variation under different microphysical conditions. These results suggest that the formation of in-cloud SOA tends to occur preferentially in smaller droplets, which partly align with the results in Sect. 3.3.1. This could be attributed to the larger unit surface area of smaller droplets, which enhances the uptake coefficient of gaseous precursors (Guo et al., 2019; Ervens et al., 2011), or to their longer atmospheric residence time, allowing for more extensive aqueous-phase oxidation of organics (Chandrakar et al., 2016; Yeom et al., 2025). In contrast, POA appeared to be more efficiently incorporated into larger droplets through in-cloud scavenging. A similar perspective was reported in studies on the in-cloud removal of BC, which suggested that 30–90% of BC is incorporated into cloud droplets through collision-coalescence processes, particularly within larger droplets where such interactions are more pronounced (Ding et al., 2025). Based on this, it is reasonable to infer that POA, sharing similar emission sources and hygroscopic properties with BC, could also be incorporated into cloud droplets through comparable processes, making it more associated with larger droplets. In 2024, both the LWC and D_e were relatively smaller and exhibited more gradual variations. Nevertheless, a trend similar to that observed in the 2023 cloud event was still evident, indicating comparable compositional responses of organic components under differing microphysical conditions.

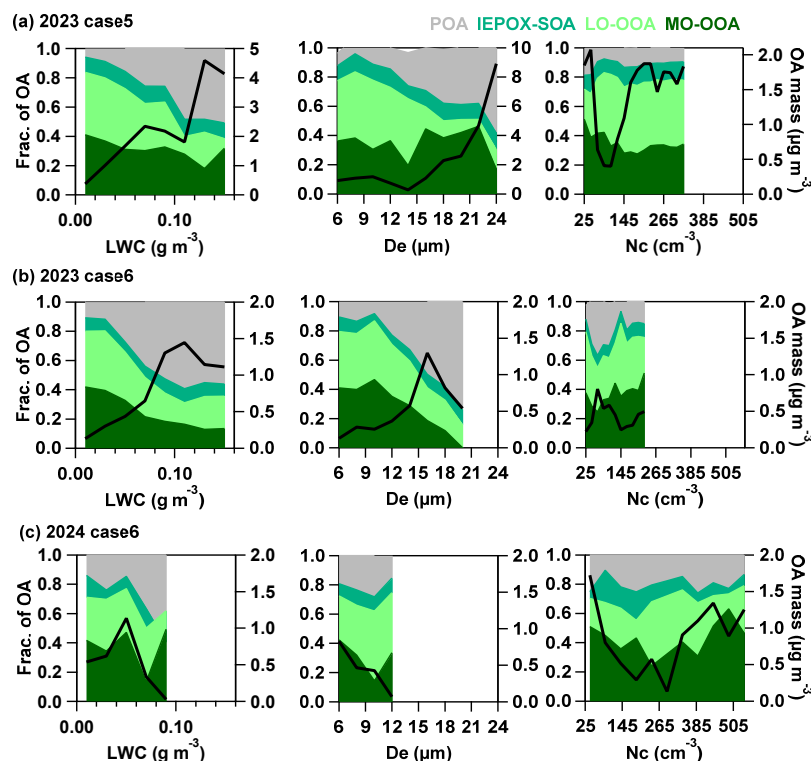


Figure 10: Mass fraction and total mass concentration of organic components as a function of cloud microphysical parameters (LWC, D_e , and N_c) during (a) case 5 in 2023, (b) case 6 in 2023 and (c) case 6 in 2024.

Beyond these compositional patterns, the observed dependencies of organic components on LWC and D_e provide valuable insights into the coupled microphysical and chemical processes governing in-cloud SOA formation. The distinct behaviour of organic components with varying LWC and D_e may also reflect differences in aqueous-phase oxidation environments within droplets of different sizes. Smaller droplets often exhibit higher oxidant concentrations and lower pH, which could promote more efficient liquid-phase oxidation and formation of oxidized secondary organics (Chakraborty et al., 2016; Ervens et al., 2011; Pye et al., 2020).

4 Conclusions

This study provides an integrated, real-time characterization of chemical and microphysical evolution during cloud events at the high-altitude SH station using two complementary cloud-droplet sampling systems coupled with aerosol chemical speciation and cloud microphysical measurements. The two field campaigns featuring nocturnal orographic clouds in autumn 2023 and long-persistence stratiform clouds in spring 2024, revealed pronounced seasonal and cloud-type-dependent differences in in-cloud processing. Across both seasons, organics dominated particle mass, whereas inorganic species (nitrate, sulfate, and ammonium) exhibited consistently high scavenging efficiencies and strong enrichment in RES particles, reflecting their high hygroscopicity and efficient activation into cloud droplets. Organic components showed distinct partitioning



behaviours under different cloud regimes: organics within INT particles during orographic clouds were generally less oxidized, while those in RES particles underwent more extensive aqueous-phase aging; in contrast, persistent cloud events favoured enhanced incorporation of LO-OOA into droplets and the release of in-cloud-formed moderately oxidized organics back to the atmosphere upon droplet evaporation.

Air-mass analyses further demonstrated substantial source-dependent variability, with polluted westerly inflow yielding the highest particle loadings and the most aged organic signatures. The clear correspondence between cloud microphysics and OA evolution, particularly the preferential formation of SOA in smaller droplets with larger surface-to-volume ratios and longer lifetimes, and the efficient scavenging of POA into larger droplets through collision-coalescence highlights the critical role of droplet-scale processes in shaping cloud chemistry. Overall, our results provide quantitative constraints on how cloud formation, aqueous-phase processing, and cloud dissipation modulate aerosol composition across seasons and cloud types. These findings offer mechanistic insights essential for improving representations of in-cloud chemical processing and aerosol-cloud-climate interactions in atmospheric models.

Data availability. The data are available upon request from the corresponding author Yele Sun (sunyele@mail.iap.ac.cn).

Author contributions. WX and YS designed the research. YZ, YZ, XP, BS, ZZ, LY, YW and SL conducted the measurements. YZ, YL, SZ and YS analysed the data. WX, GZ, DL, YK, WZ, LL, XP, ZW, XB, ME, DRW and YS reviewed and commented on the paper. YZ, WX and YS wrote the paper.

Competing interests. One of the co-authors, Dantong Liu, is a member of the editorial board of Atmospheric Chemistry and Physics.

Financial support. This work was supported by the National Natural Science Foundation of China (42330605, 42377101, 42305113), and the Strategic Priority Research Program of the Chinese Academy of Sciences (XDB0760200).

References

- Adachi, K., Tobo, Y., Koike, M., Freitas, G., Zieger, P., and Krejci, R.: Composition and mixing state of Arctic aerosol and cloud residual particles from long-term single-particle observations at Zeppelin Observatory, Svalbard, Atmos. Chem. Phys., 22, 14421-14439, 10.5194/acp-22-14421-2022, 2022.
- Bi, X., Lin, Q., Peng, L., Zhang, G., Wang, X., Brechtel, F. J., Chen, D., Li, M., Peng, P. a., Sheng, G., and Zhou, Z.: In situ detection of the chemistry of individual fog droplet residues in the Pearl River Delta region, China, J. Geophys. Res. Atmos., 121, 9105-9116, 10.1002/2016JD024886, 2016.
- Chakraborty, A., Ervens, B., Gupta, T., and Tripathi, S. N.: Characterization of organic residues of size-resolved fog droplets and their atmospheric implications, J. Geophys. Res. Atmos., 121, 4317-4332, 10.1002/2015JD024508, 2016.



- Chandrakar, K. K., Cantrell, W., Chang, K., Ciochetto, D., Niedermeier, D., Ovchinnikov, M., Shaw, R. A., and Yang, F.: Aerosol indirect effect from turbulence-induced broadening of cloud-droplet size distributions, *Proc. Natl. Acad. Sci.*, 113, 14243-14248, 10.1073/pnas.1612686113, 2016.
- Chen, J., Budisulistiorini, S. H., Itoh, M., Lee, W. C., Miyakawa, T., Komazaki, Y., Yang, L. D. Q., and Kuwata, M.: Water uptake by fresh Indonesian peat burning particles is limited by water-soluble organic matter, *Atmos. Chem. Phys.*, 17, 11591-11604, 10.5194/acp-17-11591-2017, 2017.
- Demoz, B. B., Collett, J. L., and Daube, B. C.: On the Caltech Active Strand Cloudwater Collectors, *Atmos. Res.*, 41, 47-62, 10.1016/0169-8095(95)00044-5, 1996.
- Deng, Y., Kagami, S., Ogawa, S., Kawana, K., Nakayama, T., Kubodera, R., Adachi, K., Hussein, T., Miyazaki, Y., and Mochida, M.: Hygroscopicity of Organic Aerosols and Their Contributions to CCN Concentrations Over a Midlatitude Forest in Japan, *J. Geophys. Res. Atmos.*, 123, 9703-9723, 10.1029/2017JD027292, 2018.
- Ding, S., Liu, D., Zhao, S., Wu, Y., Li, S., Pan, B., Teng, X., Li, W., Xu, W., Zhang, Y., Sun, Y., Wu, Y., Pan, X., Peng, X., Zhang, G., Bi, X., Tian, P., Liu, L., and Wang, Z.: Field Observation of Important Nonactivation Scavenging of Black Carbon by Clouds, *Environ. Sci. Technol.*, 59, 9689-9698, 10.1021/acs.est.5c00199, 2025.
- Elperin, T., Fominykh, A., and Krasovtsov, B.: Scavenging of soluble gases by evaporating and growing cloud droplets in the presence of aqueous-phase dissociation reaction, *Atmos. Environ.*, 42, 3076-3086, 10.1016/j.atmosenv.2007.12.036, 2008.
- Ervens, B., Turpin, B. J., and Weber, R. J.: Secondary organic aerosol formation in cloud droplets and aqueous particles (aqSOA): a review of laboratory, field and model studies, *Atmos. Chem. Phys.*, 11, 11069-11102, 10.5194/acp-11-11069-2011, 2011.
- Forster, P., Storelvmo, T., Armour, K., Collins, W., Dufresne, J.-L., Frame, D., Lunt, D. J., Mauritsen, T. T., Palmer, M. D., Watanabe, M., Wild, M., and Zhang, H.: The Earth's Energy Budget, Climate Feedbacks, and Climate Sensitivity, *Climate Change 2021: The Physical Science Basis. Contribution of Working Group I to the Sixth Assessment Report of the Intergovernmental Panel on Climate Change* 923–1054, 10.1017/9781009157896.009, 2021.
- Gantt, B. and Meskhidze, N.: The physical and chemical characteristics of marine primary organic aerosol: a review, *Atmos. Chem. Phys.*, 13, 3979-3996, 10.5194/acp-13-3979-2013, 2013.
- Gao, M., Zhou, S., He, Y., Zhang, G., Ma, N., Li, Y., Li, F., Yang, Y., Peng, L., Zhao, J., Bi, X., Hu, W., Sun, Y., Wang, B., and Wang, X.: In Situ Observation of Multiphase Oxidation-Driven Secondary Organic Aerosol Formation during Cloud Processing at a Mountain Site in Southern China, *Environ. Sci. Technol. Lett.*, 573-581, 10.1021/acs.estlett.3c00331, 2023.
- Gilardoni, S., Massoli, P., Giulianelli, L., Rinaldi, M., Paglione, M., Pollini, F., Lanconelli, C., Poluzzi, V., Carbone, S., Hillamo, R., Russell, L. M., Facchini, M. C., and Fuzzi, S.: Fog scavenging of organic and inorganic aerosol in the Po Valley, *Atmos. Chem. Phys.*, 14, 6967-6981, 10.5194/acp-14-6967-2014, 2014.
- Graham, E. L., Zieger, P., Mohr, C., Wideqvist, U., Hennig, T., Ekman, A. M. L., Krejci, R., Ström, J., and Riipinen, I.: Physical and chemical properties of aerosol particles and cloud residuals on Mt. Åreskutan in Central Sweden during summer 2014, *Tellus B*, 72, 1-16, 10.1080/16000889.2020.1776080, 2020.



- Guo, J., Wang, Z., Tao, W., and Zhang, X.: Theoretical evaluation of different factors affecting the HO₂ uptake coefficient driven by aqueous-phase first-order loss reaction, *Sci. Total Environ.*, 683, 146-153, 10.1016/j.scitotenv.2019.05.237, 2019.
- Guo, Z., Zhang, G., Peng, X., Sun, W., Liu, F., Li, M., Pan, X., Du, X., Wang, J., Wang, Z., Wang, X., and Bi, X.: In situ measurement evidence of selective aqueous-phase formation of ammonium, nitrate, and sulfate in clouds, *Atmos. Res.*, 108514, 10.1016/j.atmosres.2025.108514, 2025.
- Haywood, J. and Boucher, O.: Estimates of the direct and indirect radiative forcing due to tropospheric aerosols: A review, *Rev. Geophys.*, 38, 513-543, 10.1029/1999RG000078, 2000.
- Hill, K. A., Shepson, P. B., Galbavy, E. S., Anastasio, C., Kourtev, P. S., Konopka, A., and Stirm, B. H.: Processing of atmospheric nitrogen by clouds above a forest environment, *J. Geophys. Res. Atmos.*, 112, D11301, 10.1029/2006JD008002, 2007.
- Hoppel, W. A., Frick, G. M., and Larson, R. E.: Effect of nonprecipitating clouds on the aerosol size distribution in the marine boundary layer, *Geophys. Res. Lett.*, 13, 125-128, 10.1029/GL013i002p00125, 1986.
- Hu, W., Day, D. A., Campuzano-Jost, P., Nault, B. A., Park, T., Lee, T., Croteau, P., Canagaratna, M. R., Jayne, J. T., Worsnop, D. R., and Jimenez, J. L.: Evaluation of the New Capture Vaporizer for Aerosol Mass Spectrometers (AMS): Elemental Composition and Source Apportionment of Organic Aerosols (OA), *ACS Earth Space Chem.*, 2, 410-421, 10.1021/acsearthspacechem.8b00002, 2018.
- Hu, W. W., Campuzano-Jost, P., Palm, B. B., Day, D. A., Ortega, A. M., Hayes, P. L., Krechmer, J. E., Chen, Q., Kuwata, M., Liu, Y. J., de Sá, S. S., McKinney, K., Martin, S. T., Hu, M., Budisulistiorini, S. H., Riva, M., Surratt, J. D., St. Clair, J. M., Isaacman-Van Wertz, G., Yee, L. D., Goldstein, A. H., Carbone, S., Brito, J., Artaxo, P., de Gouw, J. A., Koss, A., Wisthaler, A., Mikoviny, T., Karl, T., Kaser, L., Jud, W., Hansel, A., Docherty, K. S., Alexander, M. L., Robinson, N. H., Coe, H., Allan, J. D., Canagaratna, M. R., Paulot, F., and Jimenez, J. L.: Characterization of a real-time tracer for isoprene epoxydiols-derived secondary organic aerosol (IEPOX-SOA) from aerosol mass spectrometer measurements, *Atmos. Chem. Phys.*, 15, 11807-11833, 10.5194/acp-15-11807-2015, 2015.
- Hutchings, J. W., Robinson, M. S., McIlwraith, H., Triplett Kingston, J., and Herckes, P.: The Chemistry of Intercepted Clouds in Northern Arizona during the North American Monsoon Season, *Water Air Soil Pollut.*, 199, 191-202, 10.1007/s11270-008-9871-0, 2009.
- Igawa, M. and Wang, Y.: Characteristics of Fog and Drizzle in Yokohama and in Mt. Oyama, Japan, *Water Air Soil Pollut.*, 233, 533, 10.1007/s11270-022-06012-x, 2022.
- Joo, T., Chen, Y., Xu, W., Croteau, P., Canagaratna, M. R., Gao, D., Guo, H., Saavedra, G., Kim, S. S., Sun, Y., Weber, R., Jayne, J., and Ng, N. L.: Evaluation of a New Aerosol Chemical Speciation Monitor (ACSM) System at an Urban Site in Atlanta, GA: The Use of Capture Vaporizer and PM_{2.5} Inlet, *ACS Earth Space Chem.*, 5, 2565-2576, 10.1021/acsearthspacechem.1c00173, 2021.



- Kuang, Y., Xu, W., Tao, J., Luo, B., Liu, L., Xu, H., Xu, W., Xue, B., Zhai, M., Liu, P., and Sun, Y.: Divergent Impacts of Biomass Burning and Fossil Fuel Combustion Aerosols on Fog-Cloud Microphysics and Chemistry: Novel Insights From Advanced Aerosol-Fog Sampling, *Geophys. Res. Lett.*, 51, e2023GL107147, 10.1029/2023GL107147, 2024.
- Lawrence, C. E., Casson, P., Brandt, R., Schwab, J. J., Dukett, J. E., Snyder, P., Yerger, E., Kelting, D., VandenBoer, T. C., and Lance, S.: Long-term monitoring of cloud water chemistry at Whiteface Mountain: the emergence of a new chemical regime, *Atmos. Chem. Phys.*, 23, 1619-1639, 10.5194/acp-23-1619-2023, 2023.
- Lei, L., Zhou, W., Chen, C., He, Y., Li, Z., Sun, J., Tang, X., Fu, P., Wang, Z., and Sun, Y.: Long-term characterization of aerosol chemistry in cold season from 2013 to 2020 in Beijing, China, *Environ. Pollut.*, 268, 115952, 10.1016/j.envpol.2020.115952, 2021.
- Li, J., Wang, X., Chen, J., Zhu, C., Li, W., Li, C., Liu, L., Xu, C., Wen, L., Xue, L., Wang, W., Ding, A., and Herrmann, H.: Chemical composition and droplet size distribution of cloud at the summit of Mount Tai, China, *Atmos. Chem. Phys.*, 17, 9885-9896, 10.5194/acp-17-9885-2017, 2017.
- Li, J., Zhu, C., Chen, H., Zhao, D., Xue, L., Wang, X., Li, H., Liu, P., Liu, J., Zhang, C., Mu, Y., Zhang, W., Zhang, L., Herrmann, H., Li, K., Liu, M., and Chen, J.: The evolution of cloud and aerosol microphysics at the summit of Mt. Tai, China, *Atmos. Chem. Phys.*, 20, 13735-13751, 10.5194/acp-20-13735-2020, 2020a.
- Li, T., Wang, Z., Wang, Y., Wu, C., Liang, Y., Xia, M., Yu, C., Yun, H., Wang, W., Wang, Y., Guo, J., Herrmann, H., and Wang, T.: Chemical characteristics of cloud water and the impacts on aerosol properties at a subtropical mountain site in Hong Kong SAR, *Atmos. Chem. Phys.*, 20, 391-407, 10.5194/acp-20-391-2020, 2020b.
- Liu, Q., Shen, X., Sun, J., Zhang, Y., Qi, B., Ma, Q., Han, L., Xu, H., Hu, X., Lu, J., Liu, S., Yu, A., Liang, L., Gao, Q., Wang, H., Che, H., and Zhang, X.: Characterization of fog microphysics and their relationships with visibility at a mountain site in China, *Atmos. Chem. Phys.*, 25, 3253-3267, 10.5194/acp-25-3253-2025, 2025.
- Mattsson, F., Neuberger, A., Heikkinen, L., Gramlich, Y., Paglione, M., Rinaldi, M., Decesari, S., Zieger, P., Riipinen, I., and Mohr, C.: Enrichment of organic nitrogen in fog residuals observed in the Italian Po Valley, *Atmos. Chem. Phys.*, 25, 7973-7989, 10.5194/acp-25-7973-2025, 2025.
- McCoy, I. L., McCoy, D. T., Wood, R., Regayre, L., Watson-Parris, D., Grosvenor, D. P., Mulcahy, J. P., Hu, Y., Bender, F. A. M., Field, P. R., Carslaw, K. S., and Gordon, H.: The hemispheric contrast in cloud microphysical properties constrains aerosol forcing, *Proc. Natl. Acad. Sci.*, 117, 18998-19006, 10.1073/pnas.1922502117, 2020.
- Noone, K. J., Ogren, J. A., Hallberg, A., Heintzenberg, J., Ström, J., Hansson, H.-C., Svenningsson, B., Wiedensohler, A., Fuzzi, S., Facchini, M. C., Arends, B. G., and Berner, A.: Changes in aerosol size- and phase distributions due to physical and chemical processes in fog, *Tellus B*, 44, 489-504, 10.1034/j.1600-0889.1992.t01-4-00004.x, 1992.
- O'Dowd, C. D., Facchini, M. C., Cavalli, F., Ceburnis, D., Mircea, M., Decesari, S., Fuzzi, S., Yoon, Y. J., and Putaud, J.-P.: Biogenically driven organic contribution to marine aerosol, *Nature*, 431, 676-680, 10.1038/nature02959, 2004.
- Paatero, P.: The Multilinear Engine—A Table-Driven, Least Squares Program for Solving Multilinear Problems, Including the n-Way Parallel Factor Analysis Model, *J. Comput. Graph. Stat.*, 8, 854-888, 10.1080/10618600.1999.10474853, 1999.



- Pan, B., Liu, D., Du, Y., Zhao, D., Hu, K., Ding, S., Yu, C., Tian, P., Wu, Y., Li, S., and Kumar, K. R.: Intercomparisons on the Vertical Profiles of Cloud Microphysical Properties From CloudSat Retrievals Over the North China Plain, *J. Geophys. Res. Atmos.*, 128, e2023JD039093, 10.1029/2023JD039093, 2023.
- Pierce, J. R., Croft, B., Kodros, J. K., D'Andrea, S. D., and Martin, R. V.: The importance of interstitial particle scavenging by cloud droplets in shaping the remote aerosol size distribution and global aerosol-climate effects, *Atmos. Chem. Phys.*, 15, 6147-6158, 10.5194/acp-15-6147-2015, 2015.
- Pye, H. O. T., Nenes, A., Alexander, B., Ault, A. P., Barth, M. C., Clegg, S. L., Collett Jr, J. L., Fahey, K. M., Hennigan, C. J., Herrmann, H., Kanakidou, M., Kelly, J. T., Ku, I. T., McNeill, V. F., Riemer, N., Schaefer, T., Shi, G., Tilgner, A., Walker, J. T., Wang, T., Weber, R., Xing, J., Zaveri, R. A., and Zuend, A.: The acidity of atmospheric particles and clouds, *Atmos. Chem. Phys.*, 20, 4809-4888, 10.5194/acp-20-4809-2020, 2020.
- Seinfeld, J. H., Pandis, S. N., and Noone, K. J. J. P. T.: *Atmospheric Chemistry and Physics: From Air Pollution to Climate Change*, 51, 88-90, 1998.
- Shen, X., Liu, Q., Sun, J., Kong, W., Ma, Q., Qi, B., Han, L., Zhang, Y., Liang, L., Liu, L., Liu, S., Hu, X., Lu, J., Yu, A., Che, H., and Zhang, X.: Measurement report: The influence of particle number size distribution and hygroscopicity on the microphysical properties of cloud droplets at a mountain site, *Atmos. Chem. Phys.*, 25, 5711-5725, 10.5194/acp-25-5711-2025, 2025.
- Shingler, T., Dey, S., Sorooshian, A., Brechtel, F. J., Wang, Z., Metcalf, A., Coggon, M., Mülmenstädt, J., Russell, L. M., Jonsson, H. H., and Seinfeld, J. H.: Characterisation and airborne deployment of a new counterflow virtual impactor inlet, *Atmos. Meas. Tech.*, 5, 1259-1269, 10.5194/amt-5-1259-2012, 2012.
- Sun, P., Farley, R. N., Li, L., Srivastava, D., Niedeck, C. R., Li, J., Wang, N., Cappa, C. D., Pusede, S. E., Yu, Z., Croteau, P., and Zhang, Q.: PM_{2.5} composition and sources in the San Joaquin Valley of California: A long-term study using ToF-ACSM with the capture vaporizer, *Environ. Pollut.*, 292, 118254, 10.1016/j.envpol.2021.118254, 2022.
- Sun, W., Guo, Z., Peng, X., Lin, J., Fu, Y., Yang, Y., Zhang, G., Jiang, B., Liao, Y., Chen, D., Wang, X., and Bi, X.: Molecular characteristics, sources and transformation of water-insoluble organic matter in cloud water, *Environ. Pollut.*, 325, 121430, 10.1016/j.envpol.2023.121430, 2023.
- Sun, W., Zhang, G., Guo, Z., Fu, Y., Peng, X., Yang, Y., Hu, X., Lin, J., Jiang, F., Jiang, B., Liao, Y., Chen, D., Chen, J., Ou, J., Wang, X., Peng, P. a., and Bi, X.: Formation of In-Cloud Aqueous-Phase Secondary Organic Matter and Related Characteristic Molecules, *J. Geophys. Res. Atmos.*, 129, e2023JD040355, 10.1029/2023JD040355, 2024.
- Sun, Y., Luo, H., Li, Y., Zhou, W., Xu, W., Fu, P., and Zhao, D.: Atmospheric organic aerosols: online molecular characterization and environmental impacts, *npj Clim. Atmos. Sci.*, 8, 305, 10.1038/s41612-025-01199-2, 2025.
- Twomey, S.: Pollution and the planetary albedo, *Atmos. Environ.*, 8, 1251-1256, 10.1016/0004-6981(74)90004-3, 1974.
- Wang, Z., Pan, X., Sun, Y., Xin, J., Su, H., Cao, J., Li, J., Yang, T., Liu, H., Yao, W., Xu, W., Chen, X., Zhou, W., Ma, Y., Cheng, X., Ye, J., Hu, B., Jiang, R., Wang, Z., Ge, B., Wu, L., Li, X., Li, J., Wu, Z., Kong, L., Zhu, M., Jia, J., Li, X., Fang, X., and Liu, L.: Atmospheric Boundary Layer Eco-Environment Shanghuang Observatory: An Integrated Multiscale



- Research Platform in Southeastern China for Understanding Boundary Layer Processes, Atmospheric Chemistry Feedback, and Extreme Weather–Climate Linkages, *Adv. Atmos. Sci.*, 43, 1-9, 10.1007/s00376-025-5307-7, 2025.
- 545 Xu, W., He, Y., Qiu, Y., Chen, C., Xie, C., Lei, L., Li, Z., Sun, J., Li, J., Fu, P., Wang, Z., Worsnop, D. R., and Sun, Y.: Mass spectral characterization of primary emissions and implications in source apportionment of organic aerosol, *Atmos. Meas. Tech.*, 13, 3205-3219, 10.5194/amt-13-3205-2020, 2020.
- Yeom, J. M., Fahandezh Sadi, H., Anderson, J. C., Yang, F., Cantrell, W., and Shaw, R. A.: Cloud microphysical response to entrainment of dry air containing aerosols, *npj Clim. Atmos. Sci.*, 8, 8, 10.1038/s41612-024-00889-7, 2025.
- 550 Zhang, G., Hu, X., Sun, W., Yang, Y., Guo, Z., Fu, Y., Wang, H., Zhou, S., Li, L., Tang, M., Shi, Z., Chen, D., Bi, X., and Wang, X.: A comprehensive study about the in-cloud processing of nitrate through coupled measurements of individual cloud residuals and cloud water, *Atmos. Chem. Phys.*, 22, 9571-9582, 10.5194/acp-22-9571-2022, 2022.
- Zhang, J., Lance, S., Marto, J., Sun, Y., Ninneman, M., Crandall, B. A., Wang, J., Zhang, Q., and Schwab, J. J.: Evolution of Aerosol Under Moist and Fog Conditions in a Rural Forest Environment: Insights From High-Resolution Aerosol Mass Spectrometry, *Geophys. Res. Lett.*, 47, e2020GL089714, 10.1029/2020GL089714, 2020.
- 555 Zhang, Y., Xu, W., Zhou, W., Li, Y., Zhang, Z., Du, A., Qiao, H., Kuang, Y., Liu, L., Zhang, Z., He, X., Cheng, X., Pan, X., Fu, Q., Wang, Z., Ye, P., Worsnop, D. R., and Sun, Y.: Characterization of organic vapors by a Vocus proton-transfer-reaction mass spectrometry at a mountain site in southeastern China, *Sci. Total Environ.*, 919, 170633, 10.1016/j.scitotenv.2024.170633, 2024a.
- Zhang, Z., Xu, W., Zhang, Y., Zhou, W., Xu, X., Du, A., Zhang, Y., Qiao, H., Kuang, Y., Pan, X., Wang, Z., Cheng, X., Liu, 560 L., Fu, Q., Worsnop, D. R., Li, J., and Sun, Y.: Measurement report: Impact of cloud processes on secondary organic aerosols at a forested mountain site in southeastern China, *Atmos. Chem. Phys.*, 24, 8473-8488, 10.5194/acp-24-8473-2024, 2024b.
- Zhao, X., Zhao, C., Yang, Y., Sun, Y., Xia, Y., Yang, X., and Fan, T.: Distinct changes of cloud microphysical properties and height development by dust aerosols from a case study over Inner-Mongolia region, *Atmos. Res.*, 273, 106175, 565 10.1016/j.atmosres.2022.106175, 2022.
- Zheng, Y., Cheng, X., Liao, K., Li, Y., Li, Y. J., Huang, R. J., Hu, W., Liu, Y., Zhu, T., Chen, S., Zeng, L., Worsnop, D. R., and Chen, Q.: Characterization of anthropogenic organic aerosols by TOF-ACSM with the new capture vaporizer, *Atmos. Meas. Tech.*, 13, 2457-2472, 10.5194/amt-13-2457-2020, 2020.
- 570 Zipori, A., Rosenfeld, D., Tirosh, O., Teutsch, N., and Erel, Y.: Effects of aerosol sources and chemical compositions on cloud drop sizes and glaciation temperatures, *J. Geophys. Res. Atmos.*, 120, 9653-9669, 10.1002/2015JD023270, 2015.